



## MgO-supported Ni-Sn Catalysts: Characterization and Catalytic Properties for Aqueous-phase Catalytic Reforming of Glycerol

Kiky Corneliasari Sembiring<sup>a,\*</sup>, Anis Kristiani<sup>a</sup>, Luthfiana Nurul Hidayati<sup>a</sup>, Sudiarmanto<sup>a</sup>, Fauzan Aulia<sup>a</sup>, Asif Aunillah<sup>b</sup>

<sup>a</sup> Research Center for Chemistry, Indonesian Institute of Sciences, Serpong, Tangerang Selatan, Indonesia

<sup>b</sup> Indonesian Agency for Agricultural Research and Development, Indonesian Ministry of Agriculture, Jakarta, Indonesia

\*Corresponding author: [kiky001@lipi.go.id](mailto:kiky001@lipi.go.id)

<https://doi.org/10.14710/jksa.24.6.200-205>



### Article Info

#### Article history:

Received: 2<sup>nd</sup> June 2021

Revised: 29<sup>th</sup> July 2021

Accepted: 26<sup>th</sup> August 2021

Online: 31<sup>st</sup> August 2021

#### Keywords:

Glycerol; aqueous-phase catalytic reforming; syngas; bi-metallic catalyst

### Abstract

The aqueous phase reforming (APR) of glycerol into value-added products, including H<sub>2</sub> and alkanes, is environmentally green. In this work, the conversion of glycerol into syngas was demonstrated using MgO-supported Ni-Sn catalysts. Ni species is known for its capability of converting glycerol, but the activity towards water gas shift (WGS) reaction has not been satisfied. Loading Ni-Sn onto MgO has increased the catalyst basicity, which promotes a positive effect in WGS reaction. A series of bimetallic catalysts, impregnated Ni-Sn on MgO support, was prepared with various Ni-Sn loading amounts. To better understand the behavior of prepared catalysts, they were evaluated physio-chemically through XRD, BET, and FTIR. The catalytic activity test was performed for APR in a continuous flow reactor with aqueous glycerol 10 v-% as a feedstock at a reaction temperature of 250°C. As a result, the maximum hydrogen selectivity was obtained at about 73 v-%.

### 1. Introduction

Global energy demand is increasing rapidly, and the escalation of energy consumption is driven by population and economic growth worldwide. Currently, the energy supply is primarily derived from fossil fuels, such as oil, coal, and natural gas. The progressive depletion of fossil fuel reserves has raised the concern of future renewable energy concepts. Renewable energy sources, such as solar, wind, hydro, biofuel (bioethanol, biodiesel), and hydrogen, are considered viable alternatives to conventional fossil fuels [1].

The Government of Indonesia has an ambitious plan to boost biodiesel blending gradually by 30% by 2025 [2] and continue onwards until 100%. Biodiesel has a pretty good prospect in Indonesia given the abundant availability of raw material palm oil and the advantageous properties of biodiesel as a biodegradable, non-toxic, near CO<sub>2</sub>-neutral, and environmentally friendly alternative fuel [3]. However, this increase in biodiesel production has led to another challenge of massive amounts in its by-product, glycerol, accounting for 10

wt.% of biodiesel production [4, 5]. According to the Indonesia Clean Energy Outlook 2020 Report, biodiesel production as of 2019 reached 6.9 million m<sup>3</sup>, generating 0.69 million m<sup>3</sup> of glycerol [6]. The utilization of glycerol is still limited, mainly is disposed of by incineration.

Glycerol plays an essential role as a building block for various chemicals in pharmaceutical, food, polymer industries, and fuels. For example, Cespi *et al.* [7] have reported a glycerol chlorination process for epichlorohydrin production, an epoxide and organochlorine compound for epoxy resins. Application in pharmaceutical and food industries needs more consideration due to the high purity requirement of glycerol feedstock. While crude glycerol from the biodiesel industry usually contains methanol, salts, water, and free fatty acids, it thus requires further treatments and purification. Crude glycerol has a high potential for fuels production because the high purity of feedstock is not the primary consideration, such as hydrogen (H<sub>2</sub>) production by reforming reaction [8].

H<sub>2</sub> is a clean energy carrier that can be applied in several technologies such as fuel cells to generate electricity [9]. To date, glycerol conversion into H<sub>2</sub> has been reported through steam reforming, auto thermal reforming, and aqueous-phase catalytic reforming (APR) [5, 7, 8, 9]. Among those available routes, APR is operated at a lower temperature (around 200–250°C) in comparison to the other routes, which usually require a higher reaction temperature of more than 300°C. Therefore, the APR process has attracted high interest in H<sub>2</sub> production. The mechanism of H<sub>2</sub> production via APR was pioneered by the Dumesic group [10, 11, 12]. APR can generate H<sub>2</sub> and CO<sub>2</sub> in a single step with low CO, which is essential for fuel cell applications [5]. APR process involves cleavage of C-C bonds as well as C-H bonds to form CO on the catalyst surface. Subsequently, CO is converted into H<sub>2</sub> and CO<sub>2</sub> via a water-gas shift (WGS) reaction.

Glycerol as feedstock for the APR process leads to the formation of gas and liquid products. In gas products, H<sub>2</sub>, CO, CO<sub>2</sub>, CH<sub>4</sub>, and low-chain alkanes (C<sub>2</sub>–C<sub>3</sub>) can recover. While oxygenated compounds such as alcohols, aldehydes, carboxylic acids, and diols are possibly collected in the liquid product. Fasolini *et al.* [5] have successfully collected hydroxyl acetone, glyceraldehyde, propylene, ethylene glycols, propionaldehyde, acetaldehyde, 2-propanol, 1-propanol, 2-methyl propylene, acetic, propanoic and lactic acids, methanol, and ethanol in the liquid product. To get the main product of gas, the catalyst for the APR process must perform a high activity in the cleavage of C-C bonds and WGS reaction. However, they also reported that the catalysts inhibited the cleavage of C-O bonds and methanation reaction.

In hydrocarbons reforming, Ni catalyst is commonly used and usually supported on high thermal stability oxides [13, 14]. Noble metals of Pt, Pd, Ru, Rh have shown high catalytic performance, but their high cost makes it advantageous to develop low price catalysts. Ni catalyst has shown good performance in breaking C-C, O-H, and C-H bonds in hydrocarbon reactants and facilitating the WGS reaction. Deactivation of Ni catalyst often occurred after APR caused by oxidation of the metallic Ni during reaction [13]. The addition of promoters can overcome this problem and increases hydrogen selectivity.

Sn-contained catalysts have been reported to show good activity in APR of glycerol. Previous researches [15, 16, 17, 18, 19] reported that showed good activity in H<sub>2</sub> production with more than 50% H<sub>2</sub> yield. Furthermore, the addition of Sn in the Raney nickel catalyst has reduced the sintering caused by the aqueous environment because Ni-based catalysts are vulnerable to oxidation [20]. However, the current main problem still exists in the WGS reaction to convert CO into H<sub>2</sub> and CO<sub>2</sub>. The metals supported on  $\gamma$ -Al<sub>2</sub>O<sub>3</sub> have been widely studied, but the activity towards H<sub>2</sub> production was not satisfied [21]. Ni catalysts' structural characteristics and performance are strongly influenced by the nature of support where the active site metal is deposited [22]. MgO has high thermal stability (about 700°C), maintaining nickel particles against sintering [23]. MgO has been known to have high

basicity, that property was expected to promote a positive effect in WGS reaction. The electro-donating behavior of MgO was expected to enhance H<sub>2</sub> formation so that hydrocarbon products could be limited [24]. Thus, MgO was proposed as catalyst support for this work.

In this work, a series of Ni-Sn-based catalysts supported on MgO was prepared. Subsequently, the potential application for APR of glycerol to obtain gas products rich in H<sub>2</sub> and low formation of liquid product was investigated. Ni and Sn loading amounts were selected to achieve 20 wt.% in the MgO support. The structural and morphological properties of the catalysts were characterized, and their catalytic activity towards APR of glycerol was investigated.

## 2. Experimental Section

### 2.1. Materials

Reagent-grade chemicals of glycerol ( $\geq 99.0\%$ ), Ni(NO<sub>3</sub>)<sub>2</sub>·6H<sub>2</sub>O ( $\geq 99.0\%$ ), SnCl<sub>2</sub>·2H<sub>2</sub>O ( $\geq 98.0\%$ ), MgO ( $\geq 97.0\%$ ) were purchased from Merck.

### 2.2. Catalyst Preparation

Catalysts were prepared by the incipient wetness impregnation method. The required quantity of Ni(NO<sub>3</sub>)<sub>2</sub>·6H<sub>2</sub>O, SnCl<sub>2</sub>·2H<sub>2</sub>O, and MgO were mixed in distilled water at a metal precursor and water weight ratio of 1:4 wt./vol. At 80°C, the mixture was stirred using a hot plate magnetic stirrer at 1500 rpm for 24 h. The ratio of Ni and Sn was varied (from 0 to 20 wt.%) to get a constant loading amount in MgO of 20 wt.%. The mixture was then filtered, followed by washing with deionized water. The solid material was obtained, which was ground and used as a catalyst. The catalyst was subsequently dried overnight at 105°C and calcined in an air furnace at 500°C for three hours. NiSn/MgO denotes the catalyst (x,y), x represents the loading amount of Ni, and y represents the loading amount of Sn in MgO. Before use, each prepared catalyst was treated with H<sub>2</sub> at 350°C for 3 h. Before use, each prepared catalyst was reduced in a stream of H<sub>2</sub> at 350°C for 3 h in the same steel tubular reactor used for the reaction test.

### 2.3. Catalysts Characterization

The specific surface area and catalyst porosity were measured by TriStar II 3020 Micromeritics instrument through nitrogen adsorption-desorption isotherm, at 77.3 K on liquid nitrogen. Before the analysis, the samples were degassed at 300°C for 3 h. Crystallographic phases of the synthesized catalyst were identified by X-ray diffraction (XRD) analysis using a Rigaku Smartlab diffractometer, equipped with Cu K $\alpha$  radiation at 40 kV and 30 mA and a secondary graphite monochromator with the range of  $2\theta$  was 10° – 80°. The weight loss of catalyst samples was investigated using TGA LINSEIS STA PT 1600 instrument in the air at a heating rate of 10°C.min<sup>-1</sup>. Furthermore, the types of groups and basic sites in catalyst samples were characterized using FT-IR spectroscopy in the KBr phase using a Shimadzu, Prestige-21 FT-IR Spectrometer after treated adsorption of CO<sub>2</sub>.

### 2.4. Catalytic activity test

The APR was carried out in a continuous fixed bed reactor with a total volume capacity was 25 mL. For each experiment, 2.5 g of catalyst was placed in the fixed bed reactor. Amount of 100 mL of aqueous glycerol 10 v-% was pumped into a reactor set at 250°C with liquid hourly space velocity (LHSV) of 0.75 h<sup>-1</sup>. After passed through the reactor, the reaction product was cooled through the condenser and then separated its gas and liquid product. The schematic diagram of this APR of glycerol unit is shown in Figure 1.

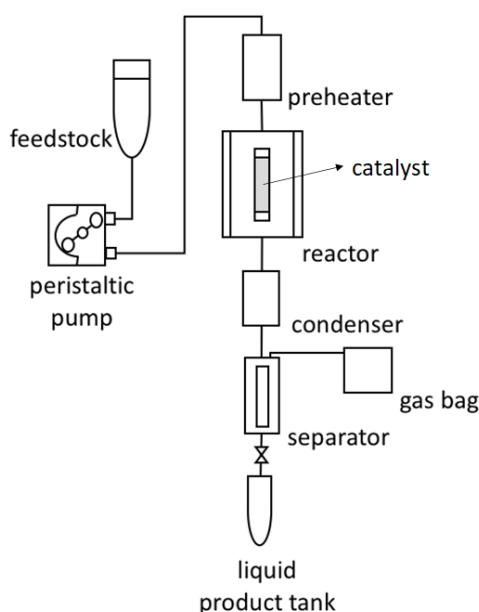


**Figure 1.** The schematic diagram of the unit for aqueous-phase catalytic reforming of glycerol

### 2.5. Product analysis

The gas products were collected in a gas bag and subsequently analyzed by GC 6890 Agilent Hewlett Packard equipped with mol sieve 5A packed column (1.83 m x 3.13 mm x 2mm, Agilent Technologies, Ltd.) with a thermal conductivity detector (TCD). The liquid product was collected in a sample vial and analyzed by gas chromatography–mass spectrometry (GC–MS) using GCMS–QP 2010 (Shimadzu Co.) equipped with HP–5MS column (30 m x 0.25 mm x 0.25 μm, Agilent Technologies, Ltd.). The initial column temperature was 70°C, and it was increased proportionally to 290°C at a rate of 15°C/min and held at 290°C for 16 min. The carrier gas, He, was provided at a constant linear velocity of 47 mL/min at 55.8 KPa. The injector and detector temperature were set at 290°C. The sample was injected at a split ratio of 50/1.

## 3. Results and Discussion

### 3.1. Characterization of Catalyst

A series of Ni–Sn bi-metallic catalysts supported on MgO have been prepared. The thermal stability of catalyst samples was characterized by TG analysis under air conditions, and the results are summarized in Figure 2. Catalyst samples were denoted NiSn compound followed by a number representing the Ni and Sn weight concentration used in preparation. Figure 2 shows that

the initial weight loss was observed at a temperature range of 80°C and 120°C that might be attributed to removing physically adsorbed water. The weight decline sharply at temperature 150°C to 400°C might reveal the release of strongly bound water molecules and organic groups, such as nitrates from catalyst metal precursors entrapped in the pores support [17]. NiSn/MgO (10,10) has the lowest total weight loss (only about 5%) in comparison with other prepared catalysts (about 15%). Although the reason remained unclear, it is considered that stronger basic sites are present in NiSn/MgO (10,10), and their amounts are more than the other catalyst samples. These strong basic sites might have higher stability. Therefore only small desorption was revealed during the TG experiment. It can be noticed in FTIR analysis that the area of the CO<sub>2</sub> adsorption band is much more significant in NiSn/MgO (10,10). Additionally, there were no appreciable thermal changes and weight loss when the samples were heated above 500°C, and it was considered as calcination temperature of the catalysts.

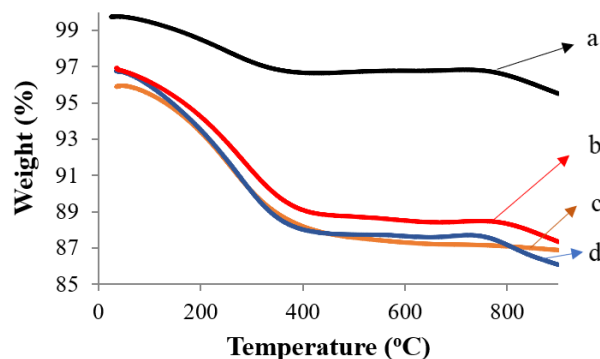


**Figure 2.** Thermogravimetric (TG) patterns of Ni–Sn impregnated on MgO with NiSn/MgO (10,10) (b) NiSn/MgO (20,0) (c) NiSn/MgO (0,20) (d) NiSn/MgO (5,15)

The ratio of Ni and Sn was varied to get a total of 20 wt.%. The prepared catalyst was analyzed its textural characteristic, such as surface area, pore-volume, and pore size by a gas adsorption isotherm; symbolized by S<sub>BET</sub>, V<sub>PORE</sub>, and D<sub>P</sub>, respectively. The textural characteristic of the catalyst samples is summarized in Table 1.

**Table 1.** Textural characteristics of Ni–Sn/MgO catalysts

Catalyst	S <sub>BET</sub> (m <sup>2</sup> /g)	V <sub>PORE</sub> (cm <sup>3</sup> /g)	D <sub>P</sub> (nm)
MgO	30.47	0.0075	2.10
NiSn/MgO (20,0)	38.61	0.0105	2.11
NiSn/MgO (10,10)	50.05	0.0134	2.11
NiSn/MgO (5,15)	33.37	0.0085	2.11
NiSn/MgO (0,20)	36.51	0.0095	2.10

The results of multiple-point BET analysis are listed in Table 1, which indicates that the BET surface was increased in the presence of metal Ni–Sn. The BET surface area increased from 30.47 m<sup>2</sup>/g to the various value depending on the Ni–Sn content, with the maximum at 50.05 m<sup>2</sup>/g. The addition of Ni–Sn metal increased catalyst surface area, total pore volume, and pore size. This increase in surface area was likely due to the

impregnation step, which was done before the MgO support was calcined. The effect of calcination-impregnation has previously been observed by Da Ros *et al.* [25]. Ni-Sn might cover the pore of the MgO support and shift the active sites to the surface of catalysts. The pore structure variation may influence the support crystalline phase change under high temperatures [16].

The XRD characterization of MgO and Ni-Sn impregnated into MgO is shown in Figure 3. The XRD patterns were observed at 18.5°, 38.0°, 58.6° (ascribed to the diffraction by the (001), (101), (110) planes) and broad and symmetrical reflection at 50.4° (ascribed to the diffraction by the (102) plane) of Mg(OH)<sub>2</sub>. The presence of the MgO periclase phase in all samples was indicated with peaks at 42.9° and 62.3°. A peak reflected niO phase at 37.5°. The intensity of this peak decreased along with a decrease in nickel content. Additionally, the reflection peaks at about 25.5°, 33.5°, and 58.9° are characteristic of SnO. SnO and NiO peaks on the samples show that the impregnation of the Ni-Sn into MgO was successful.

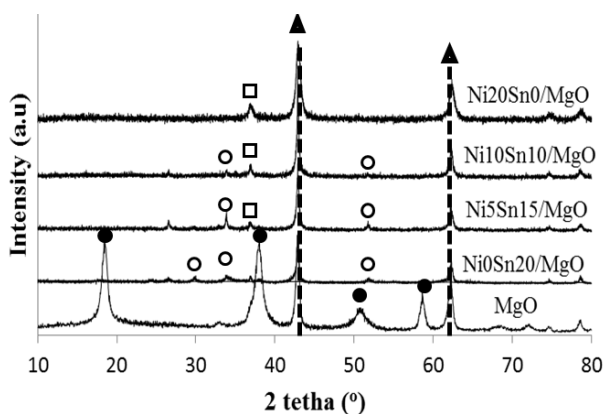


**Figure 3.** X-ray diffraction patterns for Ni-Sn/MgO with different Ni/Sn atomic ratios with ● is Mg(OH)<sub>2</sub>, ○ is SnO, □ is NiO, and ▲ is MgO

The basic properties of NiSn/MgO were observed by CO<sub>2</sub> adsorption at room temperature and then analyzed by FTIR, as presented in Figure 4. The base strength is essential in determining the catalytic WGS step, as previously studied by Bouarab *et al.* [26]. Although the catalytic reaction path cannot be determined, the interaction of H<sub>2</sub>O and basic catalyst groups is expected to give a positive effect during contact with CO as an intermediate product of the glycerol reforming process. The IR spectra obtained from Ni-Sn/MgO revealed unidentate carbonate and bidentate carbonate. Unidentate carbonate formation is a low-coordination anion that exhibits asymmetric O-C-O stretching at 1360 cm<sup>-1</sup> to 1400 cm<sup>-1</sup> and an asymmetric O-C-O stretching at 1510 cm<sup>-1</sup> to 1560 cm<sup>-1</sup>. While bidentate carbonate forms on Lewis acid-Brönsted base pairs (Mg<sup>2+</sup>-O<sup>2-</sup> pair site), and shows asymmetric O-C-O stretching at 1320 cm<sup>-1</sup> to 1340 cm<sup>-1</sup> and an asymmetric O-C-O is stretching at 1610 cm<sup>-1</sup> to 1630 cm<sup>-1</sup> [10, 27, 28].

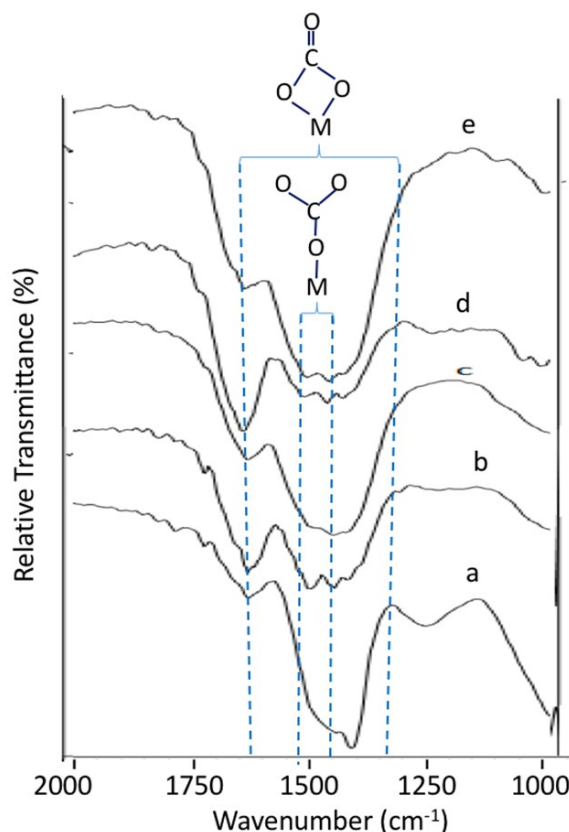


**Figure 4.** Infra-red spectra of (a) MgO, (b) NiSn/MgO (0,20), (c) NiSn/MgO (5,15) (d) NiSn/MgO (10,10), (e) NiSn/MgO (20,0)

The change of surface base sites due to the influence of Ni-Sn metal impregnation on MgO support is shown in Fig. 4. The base strength increased by impregnating Ni-Sn metal on MgO support. It was confirmed by increasing the intensity of transmittance spectra. Two bands appeared between 1400 and 1500 cm<sup>-1</sup> in all loaded Ni-Sn in MgO catalysts indicating the adsorption of CO<sub>2</sub> surfaces due to basic sites formed after Ni-Sn loading [29]. NiSn/MgO (10,10) revealed the highest increment of bidentate carbonate spectrum adsorption, which means it has the highest basicity property.

### 3.2. Catalytic activity test

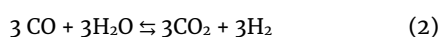
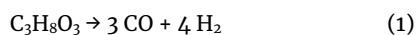
Catalytic activity test towards APR of glycerol was conducted with catalyst variation of NiSn/MgO (20,0), NiSn/MgO (10,10), NiSn/MgO (5,15), and NiSn/MgO (0,20). The result of APR reactions is summarized in Table 2. For comparison, the parent MgO support was also applied in the APR of glycerol.

**Table 2.** APR of glycerol using various MgO and Ni-Sn/MgO catalysts

Catalyst	Gas products selectivity (v-%)				
	H <sub>2</sub>	CH <sub>4</sub>	C <sub>2</sub> <sup>+</sup>	CO	CO <sub>2</sub>
MgO	0.0	0.0	66.7	0.0	33.3
NiSn/MgO (20,0)	55.7	0.2	2.2	28.3	13.6
NiSn/MgO (10,10)	72.9	0.3	15.9	6.5	4.4
NiSn/MgO (5,15)	27.2	1.1	2.6	20.9	48.2
NiSn/MgO (0,20)	59.3	1.1	4.0	35.6	0.0

From Table 2, it can be observed that the glycerol conversion is related to its transformation into gaseous products and intermediate liquid oxygenated compounds. The gas product consisted of H<sub>2</sub>, CH<sub>4</sub>, C<sub>2</sub><sup>+</sup>, CO, and CO<sub>2</sub>. Meanwhile, the liquid product analysis (data not shown) contained the remaining glycerol and conversion product of 1,2-propanediol, 2-propanone, and acetic acid.

In comparison to the catalytic activity in terms of H<sub>2</sub> selectivity, the activity of parent support MgO did not show activity in H<sub>2</sub> production. The NiSn/MgO (10,10) catalyst exhibited the most selective towards H<sub>2</sub> production from glycerol, which yielded about 72.9 v-%. It also can be seen that NiSn/MgO (10,10) catalyst produced a lower CO compound (6.5 v-%) compared to the other ones (> 20 v-%). APR consists of two-step reactions, initiated by cleaving of C–C bonds as well as C–H bonds to form CO, followed by CO conversion into H<sub>2</sub> and CO<sub>2</sub> through WGS reaction, as summarized in eq. 1 and 2. Compared to our previous works, this APR reaction using Ni-Sn/MgO gave better performance than our previous work on Cu/ $\gamma$ -Al<sub>2</sub>O<sub>3</sub> [21], which only produced 14.6 v-% of H<sub>2</sub> yield.



The high concentration of CO observed in a gas product could be caused by a low activity of the catalyst towards WGS reaction or the limitation of residence time [30, 31]. The CO content in the gas product is supposed to be a substrate for WGS reaction, as shown in equation (2). The reason for this activity remained unclear, but it is feasible that the surfaces base sites of the catalyst play an essential role in this WGS part. It can be seen that the performance of NiSn/MgO (10,10) remained the least CO content in the gas product, which means that CO reacted well to produce H<sub>2</sub>. Therefore, NiSn/MgO (10,10) catalyst with the highest basicity showed the highest H<sub>2</sub> product in this work.

#### 4. Conclusion

To study the utilization of glycerol as a by-product in biodiesel production, APR was proposed to convert glycerol into an H<sub>2</sub> rich gas product using synthesized Ni-Sn/MgO catalyst. Four types of Ni-Sn/MgO catalysts with various ratios of Ni and Sn were prepared to get the total amount of 20 wt.-% bi-metallic Ni-Sn in the catalyst. The NiSn/MgO (10,10) gave the highest H<sub>2</sub> product, yielded 72.3 v-%. Basicity property was estimated to play a role in the activity of catalyst towards APR. In this case, the high surface area of NiSn/MgO (10,10) might affect catalytic activity because the material has more surface area to form the active sites, leading to more significant activities. NiSn/MgO (10,10), which has the highest basicity property, performed the best activity in APR. This work showed that bi-metallic Ni-Sn/MgO catalyst has a good potential for H<sub>2</sub> production from glycerol.

#### Acknowledgment

The authors would like to acknowledge Aminuddin for his assistance during gas product analysis using GC-

TPD and acknowledge the funding from Research Center for Chemistry-LIPI.

#### Conflicts of Interest

The authors declare no conflict of interest.

#### References

- [1] Mandana Akia, Farshad Yazdani, Elahe Motaee, Dezhi Han, Hamidreza Arandiyani, A review on conversion of biomass to biofuel by nanocatalysts, *Biofuel Research Journal*, 1, 1, (2014), 16–25 <https://doi.org/10.18331/BRJ2015.1.1.5>
- [2] Arif Rahmanulloh, *Indonesia Biofuels Annual Report 2019*, USDA Foreign Agricultural Service, 2019
- [3] Gheorghita Mitran, Octavian Dumitru Pavel, Mihaela Florea, Daniel G. Mieritz, Dong-Kyun Seo, Hydrogen production from glycerol steam reforming over molybdena–alumina catalysts, *Catalysis Communications*, 77, (2016), 83–88 <https://doi.org/10.1016/j.catcom.2016.01.029>
- [4] Priscilla A. Selembo, Joe M. Perez, Wallis A. Lloyd, Bruce E. Logan, High hydrogen production from glycerol or glucose by electrohydrogenesis using microbial electrolysis cells, *International Journal of Hydrogen Energy*, 34, 13, (2009), 5373–5381 <https://doi.org/10.1016/j.ijhydene.2009.05.002>
- [5] Andrea Fasolini, Daniele Cespi, Tommaso Tabanelli, Raffaele Cucciniello, Fabrizio Cavani, Hydrogen from Renewables: A Case Study of Glycerol Reforming, *Catalysts*, 9, 9, (2019), 722 <https://doi.org/10.3390/catal9090722>
- [6] Agus Praditya Tampubolon, Hapsari Damayanti, Idoan Marciano, Pamela Simamora, Abdilla Alfath, *Indonesia Clean Energy Outlook 2020*, Institute for Essential Services Reform, Jakarta, 2020
- [7] D. Cespi, R. Cucciniello, M. Ricciardi, C. Capacchione, I. Vassura, F. Passarini, A. Proto, A simplified early stage assessment of process intensification: glycidol as a value-added product from epichlorohydrin industry wastes, *Green Chemistry*, 18, 16, (2016), 4559–4570 <http://dx.doi.org/10.1039/C6GC00882H>
- [8] M. S. Ardi, M. K. Aroua, N. Awanis Hashim, Progress, prospect and challenges in glycerol purification process: A review, *Renewable and Sustainable Energy Reviews*, 42, (2015), 1164–1173 <https://doi.org/10.1016/j.rser.2014.10.091>
- [9] C. Italiano, K. Bizkarra, V. L. Barrio, J. F. Cambra, L. Pino, A. Vita, Renewable hydrogen production via steam reforming of simulated bio-oil over Ni-based catalysts, *International Journal of Hydrogen Energy*, 44, 29, (2019), 14671–14682 <https://doi.org/10.1016/j.ijhydene.2019.04.090>
- [10] R. R. Davda, J. W. Shabaker, G. W. Huber, R. D. Cortright, J. A. Dumesic, A review of catalytic issues and process conditions for renewable hydrogen and alkanes by aqueous-phase reforming of oxygenated hydrocarbons over supported metal catalysts, *Applied Catalysis B: Environmental*, 56, 1, (2005), 171–186 <https://doi.org/10.1016/j.apcatb.2004.04.027>
- [11] Ivna O. Cruz, Nielson F. P. Ribeiro, Donato A. G. Aranda, Mariana M. V. M. Souza, Hydrogen production by aqueous-phase reforming of ethanol over nickel catalysts prepared from hydrotalcite

- precursors, *Catalysis Communications*, 9, 15, (2008), 2606–2611  
<https://doi.org/10.1016/j.catcom.2008.07.031>
- [12] J. W. Shabaker, G. W. Huber, R. R. Davda, R. D. Cortright, J. A. Dumesic, Aqueous-Phase Reforming of Ethylene Glycol Over Supported Platinum Catalysts, *Catalysis Letters*, 88, 1, (2003), 1–8  
<https://doi.org/10.1023/A:1023538917186>
- [13] A. Iriondo, V. L. Barrio, J. F. Cambra, P. L. Arias, M. B. Güemez, R. M. Navarro, M. C. Sánchez-Sánchez, J. L. G. Fierro, Hydrogen Production from Glycerol Over Nickel Catalysts Supported on Al<sub>2</sub>O<sub>3</sub> Modified by Mg, Zr, Ce or La, *Topics in Catalysis*, 49, 1, (2008), 46  
<https://doi.org/10.1007/s11244-008-9060-9>
- [14] D. L. Trimm, Coke formation and minimisation during steam reforming reactions, *Catalysis Today*, 37, 3, (1997), 233–238  
[https://doi.org/10.1016/S0920-5861\(97\)00014-X](https://doi.org/10.1016/S0920-5861(97)00014-X)
- [15] X. Chu, J. Liu, Minghua Qiao, J. Zhuang, Keyu Fan, Xuan Zhang, Baoning Zong, Aqueous-Phase Reforming of Ethylene Glycol to H<sub>2</sub> on Sn-Modified Rapidly Quenched Skeletal Ni-Mo Catalyst, *Chinese Journal of Catalysis*, 30, (2009), 595–600
- [16] Guoxiang Pan, Zheming Ni, Feng Cao, Xiaonian Li, Hydrogen production from aqueous-phase reforming of ethylene glycol over Ni/Sn/Al hydrotalcite derived catalysts, *Applied Clay Science*, 58, (2012), 108–113  
<https://doi.org/10.1016/j.clay.2012.01.023>
- [17] G. W. Huber, J. W. Shabaker, J. A. Dumesic, Raney Ni-Sn Catalyst for H<sub>2</sub> Production from Biomass-Derived Hydrocarbons, *Science*, 300, 5628, (2003), 2075–2077  
<https://doi.org/10.1126/science.1085597>
- [18] J. W. Shabaker, G. W. Huber, J. A. Dumesic, Aqueous-phase reforming of oxygenated hydrocarbons over Sn-modified Ni catalysts, *Journal of Catalysis*, 222, 1, (2004), 180–191  
<https://doi.org/10.1016/j.jcat.2003.10.022>
- [19] L. F. Bobadilla, A. Penkova, F. Romero-Sarria, M. A. Centeno, J. A. Odriozola, Influence of the acid-base properties over NiSn/MgO–Al<sub>2</sub>O<sub>3</sub> catalysts in the hydrogen production from glycerol steam reforming, *International Journal of Hydrogen Energy*, 39, 11, (2014), 5704–5712  
<https://doi.org/10.1016/j.ijhydene.2014.01.136>
- [20] J. W. Shabaker, D. A. Simonetti, R. D. Cortright, J. A. Dumesic, Sn-modified Ni catalysts for aqueous-phase reforming: Characterization and deactivation studies, *Journal of Catalysis*, 231, 1, (2005), 67–76  
<https://doi.org/10.1016/j.jcat.2005.01.019>
- [21] Kiky Corneliasari Sembiring, Anis Kristiani, Fauzan Aulia, Luthfiana Nurul Hidayati, Silvester Tursiloadi, Precious Metals Supported on Alumina and Their Application for Catalytic Aqueous Phase Reforming of Glycerol, *Indonesian Journal of Chemistry*, 15, 3, (2015), 269–273  
<https://doi.org/10.22146/ijc.21195>
- [22] Farzad Bastan, Mohammad Kazemeini, Afsanehsadat Larimi, Hesam Maleki, Production of renewable hydrogen through aqueous-phase reforming of glycerol over Ni/Al<sub>2</sub>O<sub>3</sub>MgO nanocatalyst, *International Journal of Hydrogen Energy*, 43, 2, (2018), 614–621  
<https://doi.org/10.1016/j.ijhydene.2017.11.122>
- [23] V. R. Choudhary, B. S. Uphade, A. S. Mamman, Large enhancement in methane-to-syngas conversion activity of supported Ni catalysts due to pre-coating of catalyst supports with MgO, CaO or rare-earth oxide, *Catalysis Letters*, 32, 3, (1995), 387–390  
<https://doi.org/10.1007/BF00813233>
- [24] Afsaneh Sadat Larimi, Mohammad Kazemeini, Farhad Khorasheh, Highly selective doped PtMgO nano-sheets for renewable hydrogen production from APR of glycerol, *International Journal of Hydrogen Energy*, 41, 39, (2016), 17390–17398  
<https://doi.org/10.1016/j.ijhydene.2016.08.006>
- [25] Simón Da Ros, Matthew D. Jones, Davide Mattia, Jose C. Pinto, Marcio Schwaab, Fabio B. Noronha, Simon A. Kondrat, Tomos C. Clarke, Stuart H. Taylor, Ethanol to 1,3-Butadiene Conversion by using ZrZn-Containing MgO/SiO<sub>2</sub> Systems Prepared by Co-precipitation and Effect of Catalyst Acidity Modification, *ChemCatChem*, 8, 14, (2016), 2376–2386  
<https://doi.org/10.1002/cctc.201600331>
- [26] R. Bouarab, S. Bennici, C. Mirodatos, A. Auroux, Hydrogen Production from the Water-Gas Shift Reaction on Iron Oxide Catalysts, *Journal of Catalysis*, 2014, (2014), 612575  
<https://doi.org/10.1155/2014/612575>
- [27] Mohammad Zangouei, Abdolsamad Zarringhalam Moghaddam, Mehdi Arasteh, The influence of nickel loading on reducibility of NiO/Al<sub>2</sub>O<sub>3</sub> catalysts synthesized by sol-gel method, *Chemical Engineering Research Bulletin*, 14, 2, (2010), 97–102  
<https://doi.org/10.3329/cerb.v14i2.5052>
- [28] J. I. Di Cosimo, V. K. Díez, C. Ferretti, C. R. Apesteguía, Chapter 1 Basic catalysis on MgO: generation, characterization and catalytic properties of active sites, in: *Catalysis: Volume 26*, The Royal Society of Chemistry, 2014,  
<http://dx.doi.org/10.1039/9781782620037-00001>
- [29] Mansur Moulavi, Kaluram Kanade, Dinesh Amalnerkar, Amanullah Fatehmulla, Abdullah M. Aldhafiri, M. Aslam Manthrammel, Synergistic surface basicity enhancement effect for doping of transition metals in nanocrystalline MgO as catalysts towards one pot Wittig reaction, *Arabian Journal of Chemistry*, 14, 5, (2021), 103134  
<https://doi.org/10.1016/j.arabj.2021.103134>
- [30] Alberto José Reynoso, Jose Luis Ayastuy, Unai Iriarte-Velasco, Miguel Ángel Gutiérrez-Ortiz, Bimetallic Pt-Co Catalysts for the Liquid-Phase WGS, *Catalysts*, 10, 8, (2020), 830  
<https://doi.org/10.3390/catal10080830>
- [31] D. Mendes, A. Mendes, L. M. Madeira, A. Iulianelli, J. M. Sousa, A. Basile, The water-gas shift reaction: from conventional catalytic systems to Pd-based membrane reactors—a review, *Asia-Pacific Journal of Chemical Engineering*, 5, 1, (2010), 111–137  
<https://doi.org/10.1002/apj.364>